# Energy dissipation of wave-uniform current over a rigid porous media with finite thickness

Jing-Hua Lin[1]   Hung-Chu Hsu[1]   Jin-Li Yu[1]   Yang-Yih Chen[1]   Guan-Yu Chen[2]

The linear wave theory and the nonlinear-unsteady porous flow model are applied to analyze the energy dissipation and the bed pore water pressure induced by the interaction of wave, uniform current and porous bottom without considering the nonlinear waves and the viscosity effect inside the boundary layer. In this model, the linear, inertial and turbulent resistances are combined into a linearized resistance coefficient and the present system can be analyzed by a linear boundary value problem. The numerical result is quite agreement with the existing experimental data. It shows that the energy dissipation is reduced by the Doppler shift and the distribution of energy loss moves to the lower relative water depth region in the wave-following current. On the other hand, the bed pore water pressure in the wave-following current is always lager than that in the pure wave and the wave-opposing current.

## 1.Introduction

The Doppler shift is the relative motion which is the change in the frequency of waves for an observer moving relative to the source. In the water wave, it represents the wave-current interaction. Non-uniform or uniform currents influence the characteristics of waves. The speed and wavelength are increased in waves encountering a favorable current and vice verse for the opposing current (Nielsen, 2012).

A lot of theoretical and experimental studies for wave-varying current interaction in the infinite and finite water depth with the smooth impermeable seabed had been performed. Typical samples are found in Longuet-Higgins and Stewart(1960,1961), Jonsson et al.(1970,1978), Jonsson(1977), Peregrine(1976), Thomas(1981,1990), Baddourand Song (1990), Groeneweg and Battjes(2003), Musumecietal.(2006), Olabarrieta et al.(2010), and Constantin and Strauss(2010). Recently, Chen et al.(2013, 2014) used the perturbation approach to analyze the high-order nonlinear wave-current interaction in 3D Lagrangian scheme, and the mass transport velocity and the particle orbit both were measured in the 1D wave-current tank. In the laboratory experiment (Huang et al.,1972), it displayed the relative importance of wave-current interaction is decided by the nondimensional parameter $U/C_0$ with $U$ as the current velocity and $C_0$ the wave speed without the current. The kinematics of the strong interaction in the wave-current motion were measured by Lai et al.(1989). Their results confirmed the critical $U/C_0$ with the currents induced the blockage of waves is -0.25. Soares and Pablo (2006) carried out an experimental study for the wave-current motion, and determined the change of wave spectra due to the coexistence of wave-current in the 3D wave basin. The experimental results showed that the energy absorbed by waves in the opposing current is impossible to continue the growth, and it is up to a certain limit, eventually resulting in wave breaking. However, the porous seabed and the energy dissipation are not considered in there existing studies.

The experiment for the wave-current interaction over a rough bed was performed by Klopman (1994). He measured the vertical profile of flow due to the wave-current interaction in the laboratory by using the Laser-Doppler-Velocimetry (LDV) system. The results pointed that the combined wave-current motion induced the mean horizontal velocity profile is significantly affected by the presence of wave. Further, Huang (2004) studied the nonlinear water wave-current interaction in rough and smooth bed with the finite depth. The rough bed induced energy dissipation can be evaluated based on his theoretical solution. In their studies, the bed is roughness and it neglects the influence of porous on the energy dissipation. Moreover, numerical simulations and observations of wave-current interaction in the real ocean environment had been mentioned in several existing studies (Wolf and Prandle, 1999; Dodet et al. 2013).

The real seabed composed of natural or the artificial porous materials can absorb the wave energy in the wave propagation and decrease the wave height due to flow resistance inside the porous medium. The phenomenon is called wave damping or energy dissipation (Karunarathna and Lin, 2006). The penetration of seabed induced the energy loss is the dominant component. Hence, the efficiency of energy loss in the porous media is significantly better than that in the rough bed based on the existing result (Lin et al.,2013).

---

[1]   International Wave Dynamics Research Center (IWDRC),Tainan Hydraulics Laboratory-National Cheng-Kung University, No.500,Sec.3,Anming Rd., Tainan, Tainan, 70955, Taiwan, R.O.C
[2]   Department of Oceanography, National Sun Yat-Sen University, No.70,Lienhai Rd, Kaohsiung, Kaohsiung, 80424, Taiwan, R.O.C

Darcy's equation related to the pressure gradient is the linear resistance model, and is commonly employed to describe the wave-porous media problem with the small seepage velocity. It is only used to the laminar flow because both the turbulent and inertial resistances are not considered. For flow through a porous and coarse sediment, the quadratic term with flow velocity and the time-dependent term are added in the original Darcy's low. It is widely applied to simulate the porous flow in the arbitrary flow regions and the wave dissipation in the wave-porous structures interaction with high permeability (Gu and Wang, 1991; Van Gent, 1995; Karunarathna and Lin, 2006).

The combined wave-current system is generally coexisted in the real ocean environment, such as the interaction between the ocean and the bayou, or the wave- tide current interaction in the open sea (Zhang et al., 2013;Chen and Chen, 2013). Hence, the experiment and theoretical studies with the seabed responses of sandy seabed under combined wave and current loading are successively developed. The energy dissipation in the wave-current-porous media is related to the bed discharge velocity and bed pore water pressure, however, these impact factors will apparently affected by Doppler shift and the properties of seabed. Understanding the energy dissipation on the wave-current-porous medium system is an important issue to design the platforms, pipelines and seawalls.

The aim of this paper is to examine the influence of combined wave-current-seabed on the energy dissipation and the bed pore water pressure in the rigid porous medium with finite thickness. The coupling equations including the complex wavenumber (the real part is the wavenumber and the imaginary part is the spatial damping coefficient) and the linearized resistance coefficient are used to numerically calculate the energy dissipation. The porous flow model, the complex dispersion relation and the numerical approach are outlined in Sec.2. The comparison between the present results and the experiment is shown in Sec.3. Finally, the influences of Doppler shift on the energy dissipation and the bed pore water pressure in the rigid porous media is displayed in Sec.4 and followed by the summary.

## 2.Boundary value problem

### 2.1 Nonlinear-unsteady porous flow model

A common nonlinear unsteady porous flow model can be shown in terms of pore pressure $p_s$ and discharge velocity $\vec{V}$ as (Corvaro et al., 2010),

$$-\nabla p_s = a\vec{V} + b\vec{V}\left|\vec{V}\right| + c\frac{\partial \vec{V}}{\partial t}. \tag{1}$$

$a$, $b$ and $c$ are empirical coefficients. The three terms in the right side of eq.(1) depend on the linear, quadratic and flow acceleration components, respectively. Three empirical coefficients can be given as,

$$a = \frac{\mu}{k_s}, b = \frac{C_d}{\rho}, c = C_m \tag{2}$$

The harmonic discharge velocity in the time domain $\vec{V} = \vec{V}_0 e^{-i\sigma t}$ with the absolute wave frequency $\sigma$ can be given and eq.(1) is derived,

$$-\nabla p_s = (a - i\sigma C_m + b\left|\vec{V}\right|)\vec{V} \tag{3}$$

Further, two nondimensional parameters are introduced as,

$$R = \frac{\rho\sigma}{\mu}k_s, \quad \beta = \frac{n + C_a(1-n)}{n^2} \tag{4}$$

Substituting eqs.(2) and (4) into eq.(3), the eq.(4) becomes as,

$$-\nabla p_s = \rho\sigma(\frac{1}{R} - i\beta + \frac{C_d}{\sigma}\left|\vec{V}\right|)\vec{V} = \rho\sigma f_0 \vec{V} \tag{5}$$

Eq.(5) is the linearized Sollit-Cross model (Sollit and Cross, 1972) in the term of the linearized resistance coefficient $f_0$. In eqs.(2)~(5), $\mu$ is the fluid dynamic viscosity, $\rho$ is the fluid density, and $C_m$ is the mass coefficient. $R$ is the permeability parameter, $k_s = \frac{n^2 d_s^2}{a_0(1-n)^3}$ is the intrinsic permeability. $\beta$ is defined as the inertia parameter, $n$ is the porosity, $d_s$ is the characteristic diameter of sediment and

$C_a$ is the spatial-averaged virtual mass coefficient. $C_d = b_0 \dfrac{1-n}{n^3 d_s}$ is the volumetric averaged drag coefficient. $a_0, b_0$ are shape factors related to the sediment properties (Nield and Bejan, 1992). Engelund (1953) suggested that $a_0$ and $b_0$ are 780 ~1500 or more and 1.8 ~ 3.6 or more, respectively. In the existing studies, $C_d$ is frequently replaced by a nondimensional parameter $C_f$ based on the following expression (Ward, 1964),

$$C_d = \frac{C_f}{\sqrt{k_s}} = \frac{C_f}{\sqrt{R}}\sqrt{\frac{\sigma}{\nu}}, \quad C_f = \frac{b_0}{n^2\sqrt{a_0(1-n)}} \tag{6}$$

Thus, eq.(4) can be adopted as,

$$-\nabla p_s = \rho\sigma(\frac{1}{R} - i\beta + \frac{C_f}{\sqrt{R\sigma\nu}}|\vec{V}|)\vec{V} \tag{7}$$

Sollitt-Cross model can be conveniently reduced as varying classic models via the simplification, such as Darcy's model ($\beta = 0$, $C_f = 0$), the modified Dagan's model ($\beta = 1/n$, $C_f = 0$) and the Dupuit-Forchheimer's model ($\beta = 0$, $C_f = 1$).

A linearized resistance coefficient $f_0$ ineq.(5) can be formulated as,

$$f_0 = \frac{1}{R} - i\beta + \frac{C_f}{\sqrt{R\sigma\nu}}|\vec{V}| . \tag{8}$$

Obviously, the right hand side of eq.(8) represents the linear, inertia and turbulent resistance, respectively. The determination of eq.(8) explains in the sec.2.3. For the natural porous seabed, the porosity doesn't exceed 0.6. For seabed consisting of uniform diameter, the porosity is 0.2545~0.4764 (Nield and Bejan, 1992). For general coastal wave conditions, wave frequency $\sigma \sim O(1)$ (rad/sec) and the seabed pressure gradient $\nabla(p_s/\gamma) \sim O(10^{-1})$, Gu and Wang (1991) recommended the linear resistance is the dominant force in the sandy seabed with $d_s < 2mm$, and inertial/turbulence force both are considered in the porous layer with $d_s > 10cm$.

## 2.2 Complex dispersion relationship

As plotted in Fig.1, the combined wave-uniform current $U$ over a rigid porous medium with finite thickness $h$ is considered in the present study. The x-axis and y-axis point horizontally forward and vertically upward, respectively. $y = 0$ and $y = -d$ are the mean still-water level and the fluid-solid interface, respectively. $y = -(d+h)$ is the porous seabed. $d$ is the mean water depth. In this study, the fluid is incompressible and inviscid, and the flow is irrotational. The rigid porous medium is consisted of homogerous, isotropic and saturated sediment.

Laplace's equation is used as the government equation in the upper fluid region ($\eta \le y \le -d$), as shown in eq.(9).

$$\nabla^2\phi = 0 \tag{9}$$

In the porous region ($-d \le y \le -(d+h)$), the porous flow is assumed as the incompressible flow. Thus, eq.(5) can be simplified as a pore water pressure $p_s$-related Laplace's equation using the continuity equation $\nabla \cdot \vec{V} = 0$ for the discharge velocity,
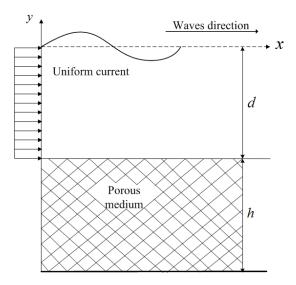
$$\nabla^2 p_s = 0 \tag{10}.$$

**Figure 1. Definition of wave-uniform current-porous medium interaction.**

The boundary conditions at the free surface, the solid/fluid interfaical bed and the bottom of porous layer are,

$$\eta = \phi_t / g \ , \ y = 0 \tag{11}$$

$$\phi_{tt} + g\phi_y = 0 \ , \ y = 0 \tag{12}$$

$$\rho\phi_t = p_s \ , \ y = -d \tag{13}$$

$$\phi_y = \frac{1}{\rho\sigma f_0} \frac{\partial p_s}{\partial y} \ , \ y = -d \tag{14}$$

$$\frac{\partial p_s}{\partial y} = 0 \ , \ y = -d \tag{15}$$

The gerenal solutions for eqs.(9)~(10) can be determined by applying boundary conditions eqs. (11)~(15) (Dean and Dalrymple, 1991; Chen et al.,2010),

$$\phi(x, y, t) = -Ux + (A\cosh k(d + y) + B\sinh k(d + y))e^{i(kx - \sigma t)} \tag{16}$$

$$p_s(x, y, t) = D\cosh k(y + d + h)e^{i(kx - \sigma t)} \tag{17}$$

with

$$D = \frac{ag\rho\sigma f_0}{\cosh kd \cosh kh(f_0 - i\tanh kd \tanh kh)(\sigma - kU)} \tag{18}$$

The complex dispersion relationship with combined wave-uniform current-porous meduim is,

$$\omega^2 - gk\tanh kd = -\frac{i}{f_0}\tanh kh(gk - \omega^2\tanh kd) \tag{19}$$

$$\omega = \sigma - k_r U \tag{20}$$

In eq.(19), $k = k_r + ik_p$ is the complex wavenumber where $k_r$ is the wavenumber and $k_p$ is the spatial damping. Eq.(20) is called as Doppler shift (or Doppler effect) where $\omega$ is the relative (intrinsic) angular frequency related to the wave number by the linear dispersion equation (Wolf and Prandle, 1999; Lin, 2008). It notes that it exists the longer relative period in the wave-following current under the same $\sigma$ and vice verse (Huang et al.,1972 ;Wolf and Prandle, 1999; Lin, 2008).

Eq.(19) can be conveniently reduced as common forms. Neglecting the Doppler shift in eq.(19), it becomes the dispersion relationship in waves travelling a porous medium (Gu and Wang,1991),

$$\sigma^2 - gk\tanh kd = -\frac{i}{f_0}\tanh kh(gk - \sigma^2\tanh kd) \tag{20}$$

Moreover, eq.(19) can be expressed as the dispersion equation in the wave-current over an impermeable seabed (Dean and Dalrymple, 1991),

$$\omega^2 - gk\tanh kd = 0 \tag{21}$$

## 2.3 Numerical approach

Based on the principle of equivalent work, the linearized resistance coefficient can be expressed as,

$$f_0 = \frac{1}{R} - i\beta + \frac{C_f}{\sqrt{R\sigma\nu}}\left|\frac{k_r D(k_r, f_0)\sinh kh}{\sigma f_0}\right| \tag{22}$$

$\bar{v} = \dfrac{k_r D(k_r, f_0)\sinh kh}{\sigma f_0}$ is the amplitude of interfacial normal seepage velocity. Eq.(19) can be separated

into the real and imaginary parts by substituting $k = k_r + ik_p$. Further, combining two equations and eq.(14) become the following coupling simultaneous-transcendental equations.

$$\begin{bmatrix} F_1 \\ F_2 \\ F_3 \end{bmatrix} = \begin{bmatrix} \mathrm{Re}(F(k_r, k_p, f_0)) \\ \mathrm{Im}(F(k_r, k_p, f_0)) \\ f_0 - (\frac{1}{R} - i\beta + \frac{C_f}{\sqrt{R\sigma\nu}}\left|\frac{k_r D(k_r, f_0)\sinh kh}{\sigma f_0}\right|) \end{bmatrix} = \begin{bmatrix} 0 \\ 0 \\ 0 \end{bmatrix} \tag{23}$$

There is no the explicit solution in this system and it could be solved by numerical approach. The Newton-Raphson method is used to iteratively find the linear resistance coefficient $f_0$, the wavenumber $k_r$ and the spatial wave attenuation coefficient $k_p$. The typical iterative expression can be shown as,

$$\begin{bmatrix} \bar{x}_1^{m+1} \\ \bar{x}_2^{m+1} \\ \vdots \\ \bar{x}_i^{m+1} \end{bmatrix} = \begin{bmatrix} \bar{x}_1^{m} \\ \bar{x}_2^{m} \\ \vdots \\ \bar{x}_i^{m} \end{bmatrix} - \begin{bmatrix} \partial F_1/\partial\bar{x}_1 & \partial F_1/\partial\bar{x}_2 & \cdots & \partial F_1/\partial\bar{x}_n \\ \partial F_2/\partial\bar{x}_1 & \partial F_2/\partial\bar{x}_2 & \cdots & \partial F_2/\partial\bar{x}_n \\ \vdots & \vdots & \cdots & \vdots \\ \partial F_i/\partial\bar{x}_1 & \partial F_i/\partial\bar{x}_2 & \cdots & \partial F_i/\partial\bar{x}_i \end{bmatrix}^{-1} \begin{bmatrix} F_1 \\ F_2 \\ \vdots \\ F_i \end{bmatrix} \tag{24}$$

and its matrix form can also be written as (Burden and Faires, 1997),

$$[\bar{x}^{m+1}] = [\bar{x}^{m}] - \left[\nabla F^m\right]^{-1}[F^m] \tag{25}$$

where matrix $[\bar{x}^{m+1}]$ and $[\bar{x}^{m}]$ are variable matrixes for $m+1$ and $m$ th step, respectively. $\left[\nabla F\right]$ is the Jacobian matrix of partial derivatives of $F$ with respect to variables $\bar{x}$.

In the iteration, Karunarathna and Lin (2006) suggested to replace $f_0$ with $f_1 - i\beta$ in the form of linear resistance coefficient, and the new form is given by,

$$f_1 = \frac{1}{R} + \frac{C_f}{\sqrt{R\sigma\nu}}\frac{\left|k_r\overline{D}(k_r, f_1)\sinh k_r d\right|}{\left|\sigma(f_1 - i\beta)\right|} \tag{26}$$

$$\overline{D}(k_r, f_1) = \frac{\bar{a}g\rho\sigma}{\cosh kd\cosh kh[1 - \frac{i}{(f_1 - i\beta)}\tanh kd\tanh kh)(\sigma - kU)]} \tag{27}$$

where $\bar{a}$ is the averaged amplitude of $ae^{-k_p x}$ over one wavelength (Gu and Wang, 1990; Karunarathna and Lin, 2006).

## 3、Comparsion with the existing experiment

The existing experiment, regular waves-uniform current travelling the sandy seabed carried out by Qi and Gao (2014), is employed to verify the theoretical solution. The test condition is shown as following with the water depth 0.5m, the sandy seabed thickness 0.5m, the mean sediment grain size ($d_s$) 0.38mm, the hydraulic conductivity ($K_s$) $1.88 \times 10^{-4} m/s$, the void ratio ($\bar{e}$) 0.771, the wave height ($H$) 10.2cm, and the wave period ($T$) 1.2 s. In this paper, the permeability coefficient ($k_s$) and the porosity ($n$) can be determined by the hydraulic conductivity and the void ratio based on the existing formulas showing as follow,

$$n = \frac{\bar{e}}{1+\bar{e}}, k_s = \frac{K_s \mu}{\gamma_w} \tag{27}$$

where $\gamma_w$ is the specific weight of pore water. The corresponging $n$ and $k_s$ can be calculated as 0.435 and $1.93 \times 10^{-11} m^2$, respectively.

The comparison with the experimental results in the wavelength is shown in Fig.2. In this illustration, another theoretical formula estimating the wavelength in the combined wave-current proposed by Zou (2004) is used,

$$L/L_0 = [1+(1+4U/C_0)^{1/2}]^2/4 \tag{28}$$

where $L$ is the wave-current interaction induced the wavelength and $L_0$ is the wavelength without the current. $C_0$ is the group velocity in the pure wave. Experimental results show that wavelength is elongated due to Doppler shift in the wave-following current field and it is shortened in the wave-opposing current flow. The present theory and experimental results match quite well. The errors between the present results and laboratory measurement are approximately 6%. The reason might due to the nonlinearity effect of wave-currnt interaction.
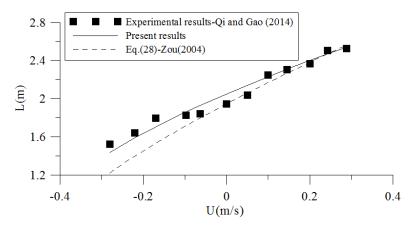


**Figure 2. Comparison of the wavelength variation calculated by the present solution and experimental data (Qi and Gao, 2014).**

## 4、Results and Disscusion

### 4.1 The influence of Doppler shift on the wavelength

The dispersion relationship with complex form, eq.(19), can be adopted as follow,

$$\omega^2 = gk \frac{-\frac{i}{f_0}\tanh kh + \tanh kd}{1 - \frac{i}{f_0}\tanh kh \tanh kd}, \omega = \sigma - k_r U \tag{29}$$

The typical case is plotted in Fig.3 with the relative thickness ratio $d/h=1$ and 0.3m water depth. Froude number $F_r$ is defined as $U/C_0$. The curve is the dispersion relationship in the wave-alone and the horizontal line is $\omega = \sigma - kU$. The intersection of two curves is the wavenumber for combined wave-uniform current-porous media interaction. The slope of straight line represents the magnitude of

uniform current and its direction. The horizontal dotted line shows $U=0$. The clockwise and counterclockwise directions represent the following and opposing current, respectively. Thus, it can be found that there are always roots in the wave-following current and the wavelength is elongated.

Conversely, there is a root in the $0<|U|<C_g$ region for the wave-opposing current (Chapman and Malanotte-Rizzoli, 1989) and where $C_g$ is the group velocity. In the real ocean environment, this situation exists near the river month region. In the mathematics, it shows that the wave length is shortened and the steepness is increased in the wave-opposing current field (Wolf and Prandle, 1999). In the physics, the wave energy is transferred into the turbulence in the wave-breaking process in the wave-opposing current when the current velocity exceeds the group velocity (Lin, 2008). A second intersection of the two curves occurs at the larger $k$, however, such wave would never existed in the $|U|>C_g$ region.
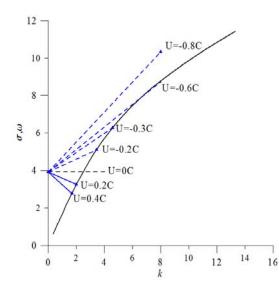


**Figure 3. Dispersion relationship in the wave-uniform current-porous media interaction with $d/h=1$ (d=0.3m ).**

## 4.2 The influence of Doppler shift on the bed pore water pressure

The nondimensional bed pore water pressure ratio $\left|\overline{p_s}/p_0\right|$ and the phase shift $\theta_p$ between the bed pore water pressure and the wave displacement in the wave-uniform current-porous medium interaction without considering the wave damping can be shown as follow,

$$\left|\frac{\overline{p_s}}{p_0}\right| = \frac{\cosh k_0 d}{\cosh kd}\alpha\frac{f_0}{\sqrt{f_0^{\,2}+(\tanh kd\,\tanh kh)^2}} \tag{30}$$

$$\theta_p = \tan^{-1}(\frac{-\tanh kd\,\tanh kh}{f_0}) \tag{31}$$

where $\overline{p_s}$ is the amplitude of bed pore water pressure under the combined wave-current loading in the porous media. $p_0 = a\gamma_w/\cosh k_0 d$ is the wave-alone induced the amplitude of bed pore water pressure in the porous medium(Chen et al.,2012). $k_0$ is the wavenumber in the wave-alone with the porous medium. $\alpha = \sigma/\omega$ is the frequency ratio. $\alpha>1$ is the wave-following current, and $\alpha<1$ shows the opposing current. Modeled parameters are listed in the Table.1. The velocities of uniform current are -0.137~1.716m/s. The relative thickness ratio $d/h$ is 0.5~2.5 with the interval 0.5.

Fig.4 shows the variation between $\left|\overline{p_s}/p_0\right|$ and $\alpha$. The magnitude of bed pore water pressure increases with that of uniform current in the wave-following current, however, it is inversely with the current velocity in the wave-opposing current. In the other words, the wave-following current induced the magnitude of bed pore water pressure is always larger than the wave alone and the wave-opposing current induced that. This phenomenon is agreement with the experimental results (Qi and Gao,2014). The liquation is related to the bed pore water pressure, and the total/local liquation is easy caused by the larger

bed pore water pressure.

The phase shift versus $\alpha$ is plotted in Fig.5. In this case, the permeability of sandy sediment is lower, and the linear resistance is the domanint component. Thus, the phase shift is smaller. It also displays that the smaller phase shift exists in the higher current velocity in the wave-following current, and the opposing results are shown for the wave-opposing current.

On the other hand, in the small current velocity $U = -0.137 \sim 0.137 m/s$ region, the variations of the bed pressure and the phase shift are proportional to the magnitude of uniform current and is the symmetry with $\alpha = 1$. The results mean that the bed pore water pressure in the wave-alone approximately equals the averaged value of summation of that in the wave-following and the wave-opposing current. The phenomenon also occurs in the phase shift.

| Table 1. The modeled parameters in the study. | |
|---|---|
| Wave amplitude a (cm) | 2.5 |
| Water depth d (m) | 0.3 |
| Seabed thickness h (m) | 0.3 |
| Soil diameter $d_s$ (mm) | 3.82 |
| Permeability $k_s$ (m$^2$) | 4.49×10$^{-9}$ |
| Porosity $n$ | 0.3 |
| Virtual mass coefficient $C_a$ | 0.46 |
| Drag coefficient $C_d = C_f / \sqrt{k_s}$ | 14928.6 |
| Coefficients $a_0 \cdot b_0$ | 570, 3 |



Figure 4. The bed pore pressure ratio $\left| p_s / p_0 \right|$ versus the frequency ratio $\alpha$ for varying $d / h$.

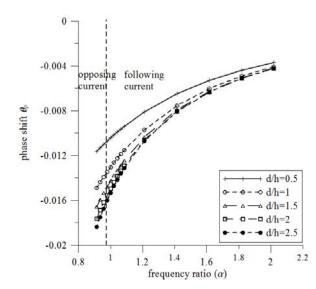**Figure 5. The phase shift $\theta_p$ versus the frequency ratio $\alpha$ for varying $d/h$.**

## 4.3 The influence of Doppler shift on the energy dissipation

The relationship between the nondimensional spatial wave damping $k_pL$ and the relative water depth $k_rd$ with $d/h=1$ and $F_r=0\sim1$ in the wave-following current is displayed in Fig.6. In this figure, the bed thickness is inversely with $d/h$. It appears that the peaks of each curves move to the shallower water region from the deeper water region due to Doppler shift. In the left side of the peak, the magnitude of energy dissipation is proportional to $k_rd$ and it is opposite to $k_rd$ in the right side of peak. Based on the existing numerical results, the magnitude of energy loss is related to the product of the pore water pressure and the vertical velocity at the interfacial boundary (Karunarathna and Lin, 2006). The interfacial vertical velocity is reduced and the bed pore water pressure is increased due to the elongation of wavelength in the wave-following current. Therefore, it obviously observes that the magnitude of energy loss in the wave-alone is significantly larger than that in the wave-following current for a certain $k_rd$. The value of energy loss approaches to a constant in the two sides of curve (ie. deeper and shallower water depth regions) and the effect of Doppler shift is not significant in two regions. A certain value of energy loss occurs at two $k_rd$. Two corresponding $k_rd$ can be defined as the alternate relative water depths and their distance is called the bandwidth. The length of bandwidth is shortened with the increase of Froude number.

The relative energy dissipation $k_p/(\sigma^2/g)$ is inversely with the relative water depth $k_rd$ ($d/h=1$), as shown in Fig.7. It points that the energy loss decreases as the increase of wavenumber in one wavelength range. The trend of theoretical solution agrees with the numerical and experimental results (Karunarathna and Lin, 2006; Corvaro, et al., 2010).

Fig.8 illustrates that the maximum spatial damping versus the relative water depth $k_rd$ with $d/h=0.5\sim2$ for $F_r=0\sim1$ in the wave-following current. It shows that the slope of the maximum energy loss is 14.4~15.2% from the subcritical flow ($F_r<1$) to the critical flow ($F_r=1$) and also implies that the influence of current on the energy dissipation would exist a upper limitation. The maximum relative energy loss $k_p/(\sigma^2/g)$ versus with the relative thickness $d/h$ with varying Froude number is plotted in Fig.9. The damping trends are the same for an arbitrary $F_r$ and are inversely with $d/h$. The results display that the only magnitude of energy dissipation is influenced by Doppler shift, and the forms of damping curve are not. The slope of energy loss in the thicker seabed ($1\leq d/h$) is significantly steeper than that in the other regions, and the value of energy loss will gradually approach as a constant for the thinner seabed ($d/h\geq2$).
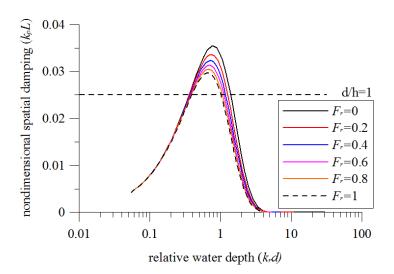
**Figure 6. The nondimensional spatial damping $k_p L$ versus the relative water depth $k_r d$ with $d/h = 1$ for varying $F_r$ in wave-following current.**
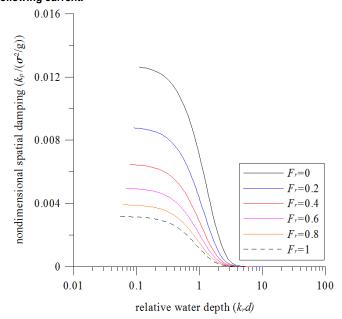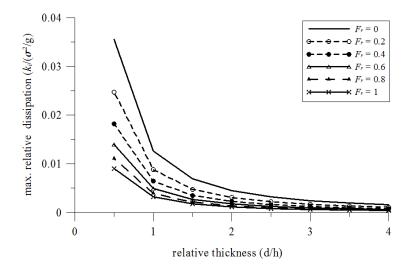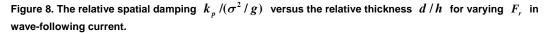


**Figure 7. The relative spatial damping $k_p /(\sigma^2 / g)$ versus the relative water depth $k_r d$ with $d/h = 1$ for varying $F_r$ in wave-following current.**

**Figure 8. The relative spatial damping** $k_p/(\sigma^2/g)$ **versus the relative thickness** $d/h$ **for varying** $F_r$ **in wave-following current.**

### 5、Summary

The theoretical solution of energy dissipation and the bed pore water pressure for the wave-uniform current-porous media based on the linear wave theory and the nonlinear-unsteady porous flow model is analyzed. The linear, inertial and turbulent resistances are combined into a linearized resistance coefficient in the Sollitt-Cross model so that the solution can be solved by a coupling linear boundary value problem. The numerical results show good agreement with the experimental data. The influences of Doppler shift on the wavelength, the bed pore water pressure and its phase lag, and the energy dissipation in the rigid porous medium are also discussed.

The energy loss depends on the product of the bed normal seepage velocity and the bed pore water pressure. These two factors are influenced by Doppler shift induced the elongation or shorten of wave length. Therefore, Doppler shift only reduces the magnitude of energy dissipation and does not change the distribution form. The maximum energy loss is found to move to the shallower water depth region in the wave-following current due to Doppler shift. Moreover, the magnification effect due to Doppler shift is found to occur in the pore water pressure. The wave-following current interaction induced the higher bed pore water pressure increases the risk of liquation of foundation of marine structures. There is the lower liquation risk in the wave-opposing current situation.

### Aknowledgements

### Reference

Baddour, R. E. and S.W. Song. 1990. Interaction of higher-order waves with uniform currents, *Ocean Engineering*, 17, 551-568.

Chapman, C. D. and P. Malanotte-Rizzoli. 1989. *Wave motions in the ocean*, Massachusetts Institute of Technology.

Constantin, A. and W. Strauss. 2010. Pressure beneath a Stokes wave, *Commun. Pure Appl. Math.*, 63, 533-557.

Corvaro, S., A. Mancinelli, M. Brocchini, E. Seta and C. Lorenzoni. 2010. On thw wave damping due to a permeable seabed, *Coastal Engineering*, 57, 1029-1041.

Chen, Y. Y., G. Y. Chen, C. H. Lin and C. L. Chou. 2010. Progressive waves in real fluids over a rigid permeable bottom, *Coastal Engineering Journal,* 52(1), 17-42.

Chen, Y. Y., H. S. Chen, C. Y. Lin and M. S. Li. 2013. Lagrangian solution for an irrotational progressive water wave propagating on a uniform current, *J. Atmos. Ocean. Technol.*, 30, 825-845.

Chen, Y. Y. and H. S. Chen. 2014. Lagrangian solution for irrotational progressive water waves propagating on a uniform current: Part 1. Fifth-order analysis, *Ocean Engineering*, 88, 546-567.

Dean, R.G. and R.A.Dalrymple. 1991. *Water wave mechanics for engineers and scientists*, World Scientific, Singapore.

Dodet, G., B. Xavier, B. Nicolas, F. B. André, N. Alphonse and R. Aron. 2013. Wave-current interactions in a wave-dominated tidal inlet, *Journal of Geophysical Research:Oceans*, 118, 1587-1605.

Engelund, F. 1953. On the laminar and turbulent flows of ground water through homogeneous sand, *Trans. Danish Acad. Tech. Sci.*, 3(4).

Gu, Z. and H. Wang. 1991. Gravity waves over porous bottom, *Coastal Engineering*, 15(5), 497-524.

Groeneweg, J. and J. Battjes. 2003. Three dimensional wave effects on a steady current. *J. Fluid Mech.*, 478, 325-343.

Huang, N. E., D. T. Chen, C. C. Tung and J. R. Smith.1972. Interaction between steady non-uniform currents and gravity waves with applications for current measurements, *Journal of Physical Oceanography*, 2, 420-431.

Huang, Z. H. 2004. Wave-current interaction in water of finite depth, Ph.D Thesis, Massachusetts Institute of Technology.

Jonsson, I. G., C. Skougaard, and J. D. Wang.1970. Interaction between waves and currents, *Proceedings of 12th Coastal Engineering Conference*, ASCE, 489-507.

Jonsson, I.G. 1977. Energy flux and wave action in gravity waves propagating on a current, *J. Hydraul. Res.*, 16, 223-234.

Jonsson, I. G., O. Brink-Kjaer and G.P.Thomas. 1978.Wave motion and set-down for waves on a shear current. *J. Fluid Mech.*, 87, 401-416.

Klopman, G. 1994. Vertical structure of the low due to waves and currents: laser-Doppler low measurements for waves following or opposing a current, *Tech. Rep. Delft Hydraulics H840.32*, Part 2.

Karunarathna, S.A.S.A and P. Lin. 2006. Numerical simulation of wave damping over porous seabed, *Coastal Engineering*, 53, 845-855.

Longuet-Higgins, M.S. and R.W. Stewart. 1960. Changes in the form of short gravity waves on long waves and tidal currents, *J. Fluid Mech.*, 8, 565-583.

Longuet-Higgins, M.S. and R.W. Stewart.1961.The changes in amplitude of short gravity waves on steady non-uniform current, *J. Fluid Mech.*, 10, 529-549.

Lai, R. J., S. R. Long and N. E. Huang. 1989. Laboratory studies of wave-current interaction: kinematics of the strong interaction, *Journal of Geophysical Research*, 94, Cll, 16201-16214.

Lin, P. 2008. *Numerical Modeling of Water Waves*, Taylor & Francis e-Library, London.

Musumeci, R. E., L. Cavallo, E., Foti and P. Scandura. 2006. Waves plus currents crossing at a right angle: experimental investigation, *J. Geophys. Res.*, 111, c07019.

Nield, D. A. and A. Bejan. 1992. *Convection in porous media*, Springer-Verlag, New York.

Nielsen, P. 2012. *Coastal and estuarine processes*, World Scientific, Singapore.

Olabarrieta, M., P. Medina and S. Castanedo. 2010. Effects of wave-current interaction on the current profile, *Coastal Engineering*, 57, 643-665.

Oi, W. G., and F. P. Gao. 2014. Responses of sandy seabed under combined waves and current: Turbulent boundary layer and pore-water pressure, *Physical Modelling in Geotechnics – Gaudin & White (Eds)*, 561~567.

Peregrine, D. H. 1976. Interaction of water waves and currents, *Adv. Appl. Mech.*, 16, 9-117.

Sollitt, C. K. and R. H. Cross. 1972. Wave transmission through permeable breakwaters, *Proc. 14th Coastal Engineering Conference*, ASCE, 1827-1846.

Soares, C. G., and H. de Pablo. 2006. Experimental study of the transformation of wave spectra by a uniform current, *Ocean Engineering*, 33, 293-310.

Thomas, G. P. 1981. Wave-current interactions: an experimental and numerical study Part 1. Linear waves, *J. Fluid Mech.*, 110, 457-474.

Thomas, G.P. 1990. Wave-current interactions: an experimental and numerical study Part 2. Nonlinear waves, *J. Fluid Mech.*, 216, 505-536.

Van Gent, M.R.A. 1995. Wave interaction with permeable coastal structure, Ph.D Thesis, Delft University.

Wolf, J. and D. Prandle. 1999. Some observations of wave–current interaction, *Coastal Engineering*, 37, 471-485.

Zou, Z. L. 2004. Water Wave Theories and Their Applications. Beijing: Science Press.

Zhang, Y., D. S. Jeng, F. P. Gao and J. S. Zhang. 2013. An analytical solution for response of a porous seabed to combined wave and current loading, *Ocean Engineering*, 57, 204-247.